OPEN

PRS GLOBAL OPEN

ORIGINAL ARTICLE
Craniofacial/Pediatric

Identification of the Peri-oral Mimic Muscles on Cadaver Slices and 3 and 7 Tesla MRI Scans

Hilde Schutte, MD*
Marvick S.M. Muradin, MD, PhD*
Karlien Seubring, MD*
Ronald L.A.W. Bleys, MD, PhD†
Frank A. Pameijer, MD, PhD‡
Antoine J.W.P. Rosenberg, MD, PhD*

Background: Decreased smile dynamics is reported as an unwanted side effect after Le Fort I osteotomies. It is assumed that this negative sequela might be caused by postoperative changes in the anatomy of peri-oral mimic muscles. Due to a lack of specific anatomical knowledge, the exact mechanism is not yet clarified. This makes prevention of the undesired changes in smile dynamics difficult. The first aim of this study is to increase basic anatomical and radiological MRI knowledge of the peri-oral mimic muscles. The second aim is to investigate if 7 Tesla MRI scans are better suited to identify these muscles than 3 Tesla MRI scans.
Methods: Eleven peri-oral mimic muscles were chosen as subjects of the present study. Three and 7 Tesla MRI scans of a cadaver head were made. The same head was cut in axial slices using a cryomacrotome. Every second slice was digitally photographed. A three-dimensional model was created utilizing EMAC software, which served as gold standard for the identification and comparison of the chosen peri-oral mimic muscles on both MRI scans.
Results: All predetermined peri-oral mimic muscles could be identified in the cadaver head, and a detailed radiological atlas was created. The ease of identification and separation of the peri-oral mimic muscles was significantly higher on the 7 Tesla MRI than on the 3 Tesla MRI scan ($P < 0.001$).
Conclusion: A 7 Tesla MRI scanner offers great improvement in the identification of peri-oral mimic muscles compared with a 3 Tesla scanner. *(Plast Reconstr Surg Glob Open 2022;10:e4113; doi: 10.1097/GOX.0000000000004113; Published online 15 February 2022.)*

INTRODUCTION

Mimetic muscles of the face play an important role in the expression of emotions, making them salient in nonverbal communication.[1,2] Being located around the eyes, nose, and mouth, they function as dilatators and sphincters of these orifices.

Research has shown that facial expressions might change after surgery.[3–5] A frequently reported side effect after surgery, especially the Le Fort I osteotomy, is the smile, which has been demonstrated to be less wide after a Le Fort I osteotomy.[3–5] Patients experience this change in facial expressions as disturbing, because of the negative influence on social interaction and perception.[3] Unfortunately, prevention of this unwanted side effect is difficult, as the exact mechanism remains unclear.

Up until now, it has been assumed that altered facial expressions might be caused by a disturbance in the normal anatomy of mimic muscles.[3,5] If during surgery mimic muscles are detached at their origin or insertion or are being severed without repositioning them at the right place, the strength and the position can be different after healing. Positional changes might change the vector in which the muscles function during contraction. Both, impaired strength and changes of the functional vector, might negatively affect muscle function, leading to altered facial expressions.[5]

This means that, during surgery, reattachment of mimic muscles to the correct anatomical site and maintaining the correct vector of movement and strength seems paramount to prevent undesirable effects of facial expression. This concept is supported by 2D research which showed

*From the *Department of Maxillofacial Surgery, University Medical Center Utrecht, Utrecht, The Netherlands; †Department of Functional Anatomy, University Medical Center Utrecht, Utrecht, The Netherlands; and ‡Department of Radiology, University Medical Center Utrecht, Utrecht, The Netherlands.*

Received for publication October 13, 2021; accepted December 3, 2021.

DOI: 10.1097/GOX.0000000000004113

Disclosure: *The authors have no financial interest to declare in relation to the content of this article.*

Related Digital Media are available in the full-text version of the article on www.PRSGlobalOpen.com.

improvement of nasolabial dynamics after using a muco-musculo-periosteal repositioning of the nasolabial mimic muscles after Le Fort I osteotomies.[6,7]

For a complete understanding of this mechanism, detailed knowledge of the normal anatomy of the mimic muscles (including their attachments at origin and insertion, their vectors of movement) and the imaging possibilities of these parameters by magnetic resonance imaging (MRI) are considered essential.

However, there remains a paucity of knowledge about the exact 3D radiological anatomy of the peri-oral mimic muscles,[8,9] and the possibilities to make this visible using MRI imaging. Mimic muscles are thin and tiny structures, overlapping and intermingling with each other. This makes it difficult to identify them as separate entities on the regularly used 3 Tesla MRI scans.[8] It is thought that this cumbersome identification of the exact anatomy of the mimic muscles on 3 Tesla MRI scans[8] might be the reason why the specific mechanisms causing altered facial expression, like a decrease in smiling dynamics after le Fort I osteotomies, remains unknown.

The use of 7 Tesla MRI scans, however, might lead to new insights. Seven Tesla MRI scans have been proven to give a more detailed display of anatomical structures for other parts of the human body.[10–13] Without doubt, research is needed to find out if using 7 Tesla MRI scans also improves diagnostics of the mimic muscles and, in particular, the peri-oral mimic muscles.

The purpose of the present study was twofold. The first aim was to increase basic anatomical and radiological MRI knowledge of the peri-oral mimic muscles. A detailed atlas will be provided, pointing out the mimic muscles on photographs of anatomical slices of a cadaver head and corresponding images of 3 and 7 Tesla MRI scans. The second aim was to investigate if a 7 Tesla MRI scanner could improve identification of the complete course of individual peri-oral mimic muscles, compared with a 3 Tesla MRI scanner.

Takeaways

Question: Definition of mimic musculature on anatomy specimen, 3 tesla MRI and 7 Tesla MRI.

Findings: Superior imaging of mimic musculature on 7 Tesla MRI, by which a detailed three-dimensional radiological atlas was created.

Meaning: This article presents a good overview of the exact anatomical position of the peri-oral mimic muscles from origin to insertion and demonstrates that using a 7 Tesla MRI scanner, compared with a 3 Tesla MRI scanner, considerably improves the identification of individual peri-oral mimic muscles in their course from origin to insertion.

MATERIALS AND METHODS

The peri-oral mimic muscles of interest were determined for the present study and divided into four groups:

1. Muscles that contribute to the elevation of the upper lip:
   - a. zygomaticus major and minor muscles
   - b. levator labii superioris muscle
   - c. levator labii superioris alaeque nasi muscle
   - d. levator anguli oris muscle
2. Muscles that close the lip:
   - a. orbicularis oris muscle
   - b. mentalis muscle
3. Muscles that contribute to the depression of the lower lip:
   - a. depressor labii inferioris muscle
   - b. depressor anguli oris muscle
4. Muscles that widen the oral fissure by moving the modiolus posterio-laterally:
   - a. buccinator muscle
   - b. risorius muscle

One cadaver head (woman, age 69, no known disruption of the facial anatomy, and without any known metal implants) was obtained from the Department of Anatomy, University Medical Center Utrecht, the Netherlands. The head was derived from a body that had entered the department of anatomy through a donation program. Written informed consent had been obtained during lifetime, permitting use of the entire body for educational and research purposes.

A total of 10 MRI scans of the cadaver head were made by two different technicians, five using a 3 Tesla MRI scanner (Philips Medical Systems, Best, The Netherlands) and five using a 7 Tesla MRI scanner (Philips Healthcare, Cleveland OH, USA). Because no standardized protocols were available for imaging the mimic muscles, the MRI scans were made with different settings based on clinical experience of the technician for the 3 Tesla MRI scanner and based on the experimental experience of the technician for the 7 Tesla MRI scanner. (**See table, Supplemental Digital Content 1**, which displays MRI scanner settings. Settings were chosen based on clinical experience of the technician for the 3 Tesla MRI scanner and based on the experimental experience of the technician for the 7 Tesla MRI scanner. Of the 3 Tesla MRI scans, number 4 provided the best imaging, and of the 7 Tesla MRI scans, number 2 provided the best imaging, and these were used for the study. **http://links.lww.com/PRSGO/B928.**) Two MRI scans, with the most similar settings to facilitate comparison, were selected. In both MRI scanners, the cadaver head was vertically positioned. The scanning direction was transverse. Sagittal and coronal slices were reconstructed, and a three-dimensional model was created within RadiAnt software (RadiAnt DICOM Viewer, version 4.1.6.16895, Medixant, Poznan, Poland).

After obtaining the 3 and 7 Tesla MRI scans of the cadaver head, the head was frozen in a carboxymethylcellulose gel at − 25°C. The frozen cadaver head was cut in consecutive transverse sections using a heavy-duty sledge cryomacrotome (CMX3600 XP; Leica Biosystems, Nussloch, Germany). A total of 5.082 slices with a thickness of 0.025 mm were obtained. Every second slice of transversely cut frozen cadaver head was photographed using a fixed digital camera (DF450C; Leica Microsystems Ltd, Heerbrugg, Switzerland). To facilitate comparison between the digital photographs and the 3 and 7 Tesla MRI scans, the MRI scans were converted using multiplanar reconstruction to equalize the slice direction of the cadaver head.

To analyze anatomical data from the digital photographs, coronal and sagittal plane images were reconstructed from the original transverse photographs of the sliced cadaver head and a 3D model was created by using enhanced multiplanar reformatting along curves (EMAC) software (E-MAC Group, Department of Information and Computing Sciences, Utrecht University, Utrecht, The Netherlands). By using an interactive image sequence viewer and EMAC together, the coronal, transversal and sagittal planes could be synchronized and shown as a movie-like animation of consecutive photographs in the plane of choice. Detailed anatomic information was acquired through the aforementioned method, making the anatomical photographs the golden standard reference in case of uncertainties in the identification of the peri-oral mimic muscles on 3 or 7 Tesla MRI scans.

Identification of the peri-oral mimic muscles was carried out on the digital photographs as well as on the 3 and 7 Tesla MRI scan. Each peri-oral mimic muscle was identified separately within the EMAC software on the synchronized anatomical photographs. The effort to identify and isolate the origins and insertions of the peri-oral mimic muscles on both 3 and 7 Tesla MRI scans was tested separately for both types of scans. Every mimic muscle was identified after consensus with all authors. The results of both sets of tests were compared with each other.

The comparison between the 3 and 7 Tesla MRI scans was expressed in the degree of ease with which a muscle could be identified and separated (ie, identified and isolated from other muscles, and was scored into three groups: no, moderate, or good. Good identification meant that finding the origin or insertion was unchallenging. Good separation meant that the origin or insertion could be well delimited from other tissues. Examples of the classification system are added in the supplementary data. [**See figure, Supplemental Digital Content 2**, which displays examples of the classification system for identification of mimic muscles. From left to right showing good identification and separation of the origin of the buccinator muscle (A); moderate identification and separation of the insertion of the risorius muscle (B); moderate identification but no separation of the origin of the depressor labii inferioris muscle (C); and no identification or separation of the origin of the levator labii superioris aleque nasi muscle (D). **http://links.lww.com/PRSGO/B929**.] Statistical analysis of these results was performed using the Wilcoxon Signed-Rank test. *P* values less than 0.05 were used as threshold for significance.

RESULTS

The scores regarding the degree of ease with which a muscle could be identified and separated from the other muscles on both MRI scans are listed in Table 1.

All the eleven predetermined peri-oral mimic muscles could be identified on the anatomical photographs of the cadaver head, although the risorius muscle was hardly noticeable. As the zygomaticus major and minor muscles were intermingled, and not separable from each other, no distinction will be made, and they will be referred to as "zygomatic muscle."

Identification of the origins and insertions was considered easier for all the mimic muscles on the 7 Tesla MRI scan. All identifications were scored as "good" on the 7 Tesla MRI scan, except for the risorius muscle, of which the origin was not identifiable. On the 3 Tesla MRI scan, only the zygomaticus muscle, the origin of the buccinators muscle, and the origin of the levator labii superioris muscle scored "good" for identification. All other muscles scored "moderate" for identification. Additionally, it was impossible to identify the origin of the levator labii superioris alaeque nasi muscle, and the origin of the risorius muscle on the 3 Tesla MRI scan, because these appeared to be too thin.

Separation was also considered to be easier on the 7 Tesla MRI scan. Separation of all muscles scored "good" on the 7 Tesla MRI scan, except for the origin of the depressor anguli oris muscle, which was scored as "moderate," and the origin of the risorius muscle, which was not separable. For the 3 Tesla MRI scan, however, only separation of the zygomaticus muscle and separation of the origin of the buccinator muscle were scored "good," and all the other muscles scored "moderate." Moreover, separation was not possible for the risorius muscle, the origin of the depressor anguli oris muscle, the depressor labii inferioris muscle, and the origin of the levator labii superioris muscle on the 3 Tesla MRI scan.

Differences between the 3 Tesla MRI scans and the 7 Tesla MRI scans in the degree of ease with which a muscle could be identified and separated from the other muscles were highly significant ($P < 0.001$). A summarizing table with these results can be found in Supplemental Digital Content 3. [**See table, Supplemental Digital Content 3**, which displays the results of the ease of identification and separation for all the insertions and origins of 10 predetermined peri-oral mimic muscles (in total 20 items scored for both scans). Significance was tested by the Wilcoxon Signed-Rank test. *Statistically significant ($P < 0.05$). **http://links.lww.com/PRSGO/B930**.]

By identifying the mimic muscles on the 7 Tesla MRI scans, a three-dimensional anatomical MRI atlas could be created. Radiological images in three directions (transversal, sagittal, and coronal), depicting the 11 predetermined mimic muscles are provided in Figures 1–3. A comparison of the identification of the mimic muscles on the cryomacrotome photograph and the 7 and 3 Tesla MRI scans is provided in Figure 4.

Table 1. Assessment of Predetermined Peri-oral Muscles regarding Identification and Separation

Muscle	Origin	Insertion	Identification and Separation: 3 Tesla MRI	Identification and Separation: 7 Tesla MRI	Comments	Direction of Movement
Muscles with a lip lifting function						
Zygomaticus muscle	Zygomatic arch	Modiolus	Origin: good identification, good separation Insertion: good identification, good separation	Origin: good identification, good separation Insertion: good identification, good separation	Zygomaticus muscle with triangular shape at origin on zygomatic arch and clearly visible bifid insertion.	Elevates angle of mouth by drawing cranially and laterally
Levator labii superioris muscle	Medial infra-orbital margin, cranial of infra-orbital foramen, fibers attached to maxillary and zygomatic bone	Skin and lateral part of upper lip, blending with orbicularis oris	Origin: good identification, moderate separation Insertion: moderate identification, moderate separation	Origin: good identification, good separation Insertion: good identification, good separation	Connection between levator labii superioris an levator labii superioris aleque nasi clearly visible on 7 Tesla MRI.	Elevates upper lip by drawing cranially
Levator labii superioris aleque nasi muscle	Upper part of frontal process of maxillary bone	Lateral part of upper lip, blending with orbicularis oris and levator labii superioris	Origin: no identification, no separation Insertion: moderate identification, moderate separation	Origin: good identification, good separation Insertion: good identification, good separation	Levator labii superioris aleque nasi too thin to be identified at origin on 3 Tesla MRI.	Elevates upper lip by drawing cranially
Levator anguli oris muscle	Canine fossa of maxillary bone, immediately caudal of infraorbital foramen	Modiolus intermingling with fibers of zygomaticus orbicularis oris and depressor anguli oris	Origin: moderate identification, moderate separation Insertion: moderate identification, moderate separation	Origin: good identification, good separation Insertion: good identification, good separation	Complete course of levator anguli oris clearly visible with more detailed outline and more contrast on 7 Tesla MRI.	Elevates angle of mouth by drawing medially
Muscles to close the lips						
Orbicularis oris muscle	Mouth encircling muscle consisting of own fibers, supplemented with fibers from buccinator, levator anguli oris, depressor anguli oris, levator labii superioris, depressor labii inferioris, zygomaticus minor and major	Skin around upper and lower lip	Origin: moderate identification, moderate separation Insertion: moderate identification, moderate separation	Origin: good identification, good separation Insertion: good identification, good separation	Marginal part of orbicularis oris clearly visible on 7 Tesla MRI as images are more detailed with more contrast.	Closes and pouts lips
Mentalis muscle	Incisive fossa of anterior part of mandible	Skin and soft tissue of chin	Origin: moderate identification, moderate separation	Origin: good identification, good separation	More detailed images with more contrast, connection of mentalis with skin and soft tissue of chin clearly visible on 7 Tesla MRI.	Elevates and wrinkles skin of chin, protrudes lower lip, raises central portion of lower lip by upward and inward movement of soft tissue of chin
Muscles resulting in downward movement of the lips						
Depressor labii inferioris muscle	Oblique line of mandible between symphysis and mental foramen, continuous with platysma	Skin of lower lip, blending with orbicularis oris	Origin: moderate identification, no separation Insertion: moderate identification, no separation	Insertion: good identification, good separation Insertion: good identification, good separation	Anatomical position where depressor labii inferioris connects with orbicularis oris and soft tissue of lip clearly visible on 7 Tesla MRI, due to lack of contrast not visible on 3 Tesla MRI.	Depresses lower lip
Depressor anguli oris muscle	Oblique line of mandible, continuous with platysma	Modiolus, continuous with orbicularis oris, risorius, and levator anguli oris	Origin: moderate identification, no separation Insertion: moderate identification, moderate separation	Origin: good identification, moderate separation Insertion: good identification, good separation	Due to lack of contrast on 3 Tesla MRI separation of depressor anguli oris not possible.	Depresses of angle of mouth

(Continued)

Table 1. (*Continued*)

Muscle	Origin	Insertion	Identification and Separation: 3 Tesla MRI	Identification and Separation: 7 Tesla MRI	Comments	Direction of Movement
Muscles to widen the lip closure by moving the modiolus posterio-laterally						
Buccinator muscle	Alveolar processes of maxilla and mandible and pterygomandibular raphe	Modiolus, blending with orbicularis oris	Origin: good identification, good separation Insertion: moderate identification, moderate separation	Origin: good identification, good separation Insertion: good identification, good separation	Gathering of buccinator with orbicularis oris, depressor anguli oris, levator anguli oris and zygomaticus major within the modiolus clearly visible on 7 Tesla MRI	Pulls back angle of mouth, flattens cheek area
Risorius muscle	Parotideomasseteric fascia / SMAS	Modiolus, skin at angle of mouth	Origin: no identification, no separation Insertion: moderate identification, moderate separation	Origin: no identification, no separation Insertion: good identification, good separation	Insertion of the risorius is visible on both 3 and 7 Tesla MRI. Origin not visible.	Draws back angle of mouth

The degree of ease with which a muscle could be identified and separated from the other muscles was divided into three groups: no identification or separation, moderate identification or separation, and good identification or separation. SMAS: superficial musculoaponeurotic system.

DISCUSSION

Imaging of the mimic muscles using MRI scanners has not been the subject of many research projects in the past. There is a limited number of publications dealing with MRI of facial muscles.[9,14] Most of these articles describe changes in facial muscles related to neuromuscular diseases or methods to quantify these changes for prognostic purposes.[9,15] Often, these articles focus on masticatory and major facial muscles, such as the masseter and the buccinator, instead of the much smaller peri-oral mimic muscles.

To the best of our knowledge to this date, only one article could be found that provided a systematic radiological description of facial muscle anatomy and the musculoaponeurotic system in general and not in the context of any pathology. The results were comprehensively presented in an MRI atlas. The authors argued that this study was done to fill up a lack of anatomical knowledge from a radiological point of view and to fulfill their desire for better anatomic accuracy. They expressed the hope that their atlas could be helpful to make clinicians more confident in identifying facial muscles on MRI scans and to make more accurate diagnoses resulting in better treatment options.[8] The MRI scanner used for this study was a 3 Tesla MRI scanner, and although 18 of 20 facial muscles were identified, only nine were defined as "well seen." This poses questions about the accuracy of the diagnostic process using 3 Tesla MR Images.

Additionally, it raises the question whether imaging with a higher magnetic field strength scanner could improve the identification of the mimic muscles. Recent studies support this idea: It has been shown that anatomical structures can be captured in more detail, thereby improving diagnostics, when using a 7 Tesla MRI scanner.[10,11] The scientific focus of the 7 Tesla MRI scanner has already moved toward clinical application for several indications.[10,11]

To date, these indications do not include imaging of the mimic muscles, as the mimic muscles have never been the topic of any 7 Tesla MRI study before. To the best of our knowledge, this is the first study that was performed to find out whether imaging with a 7 Tesla MRI scanner could improve the separate identification of the mimic muscles compared with imaging with a 3 Tesla MRI scanner. The present study demonstrates promising results on that matter.

The present study was performed both with a clinical and a technical motive. The best technical settings of imaging with a 7 Tesla MRI scanner are found in Supplemental Digital Content 1 (**see Supplemental Digital Content 1**, which displays MRI scanner settings. Settings were chosen based on clinical experience of the technician for the 3 Tesla MRI scanner and based on the experimental experience of the technician for the 7 Tesla MRI scanner. Of the 3 Tesla MRI scans, number 4 provided the best imaging, and of the 7 Tesla MRI scans, number 2 provided the best imaging, and these were used for the study. http://links.lww.com/PRSGO/B928.). The scanner settings were empirically estimated. As these settings were used on a cadaver head, translation of these settings to patients should be done with great caution. Further research is required to create standardized MRI scanning protocols.

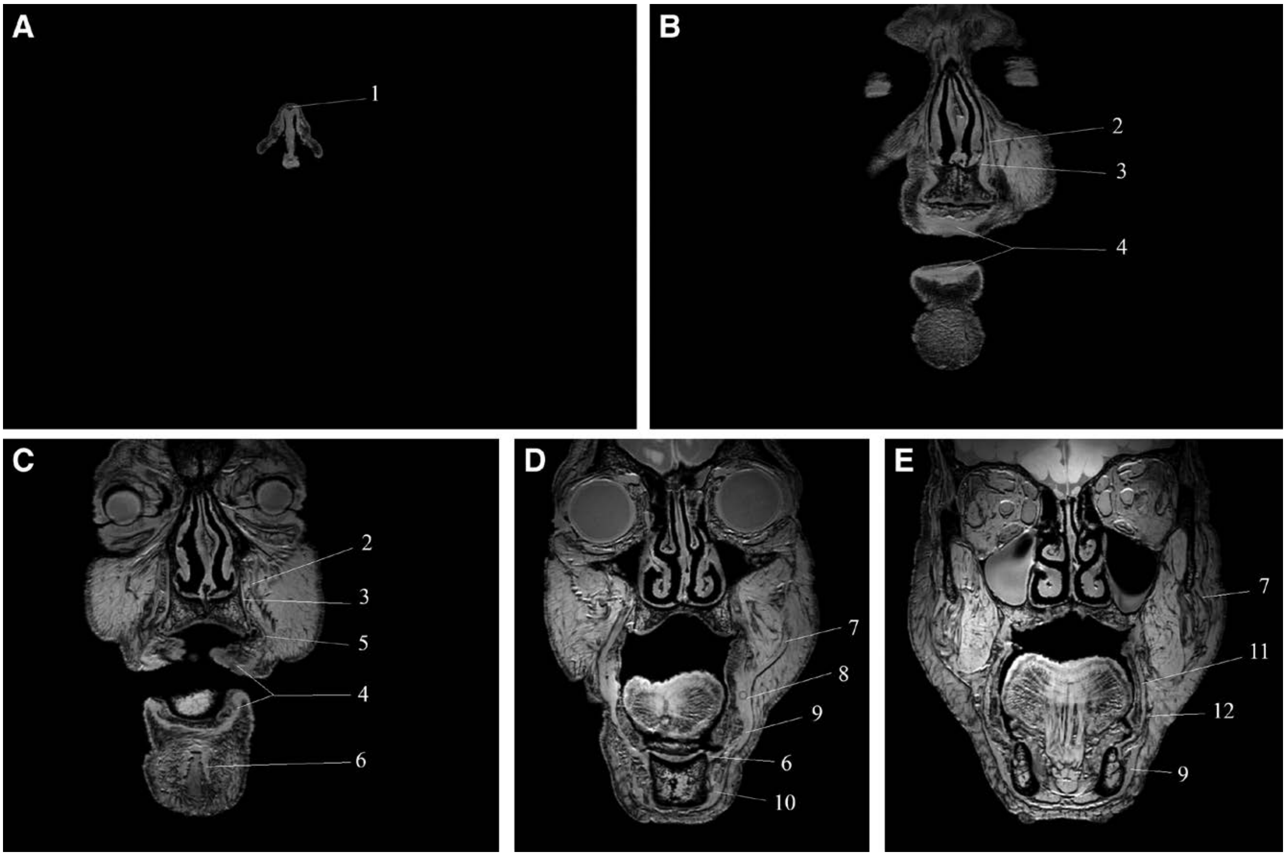

Fig. 1. Transversal. Consecutive slices from caudal to cranial in consecutive order of the 7 Tesla MRI scans (A-E). Legend of mimic muscles: 1. Mentalis muscle; 2. Depressor labii inferioris muscle; 3. Depressor anguli oris muscle; 4. Orbicularis oris muscle; 5. Modiolus region; 6. Risorius muscle; 7. Buccinator muscle; 8. Zygomaticus muscle; 9. Levator labii superioris aleque nasi muscle; 10. Levator labii superioris muscle; 11. Levator anguli oris muscle; 12. Nasalis muscle.

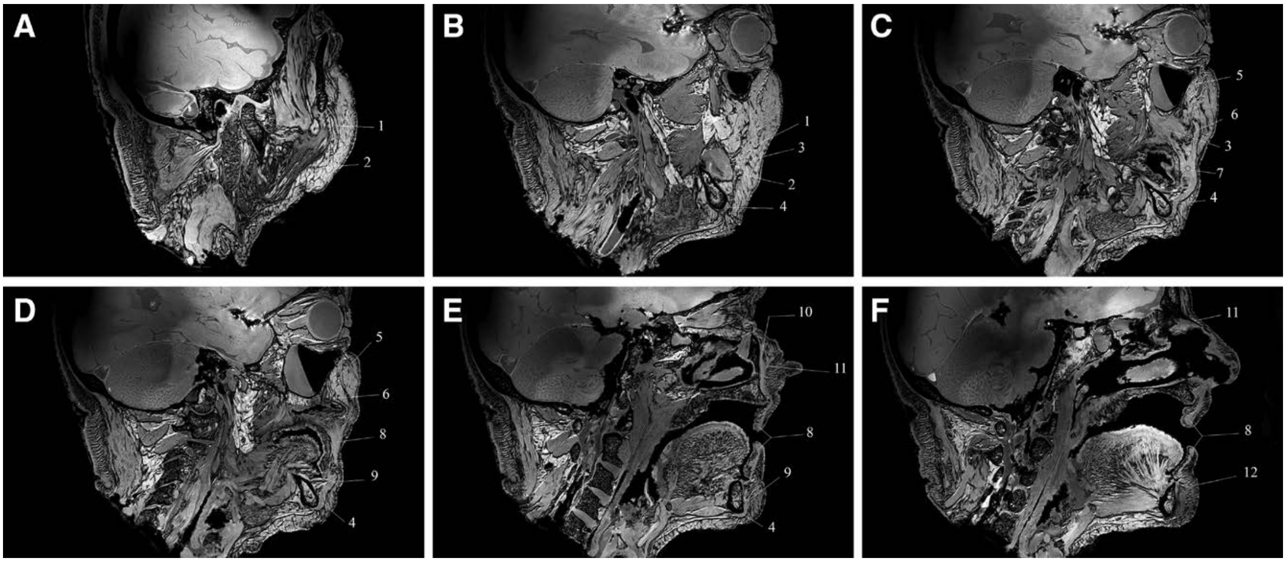

Fig. 2. Sagittal. Consecutive slices from lateral to medial in consecutive order of the 7 Tesla MRI scans (A-F). Legend of mimic muscles: 1. Zygomaticus muscle; 2. Risorius muscle; 3. Buccinator muscle; 4. Depressor anguli oris muscle; 5. Levator labii superioris muscle; 6. Levator anguli oris muscle; 7. Modiolus region; 8. Orbicularis oris muscle; 9. Depressor labii inferioris muscle; 10. Levator labii superioris aleque nasi muscle; 11. Nasalis muscle; 12. Mentalis muscle.

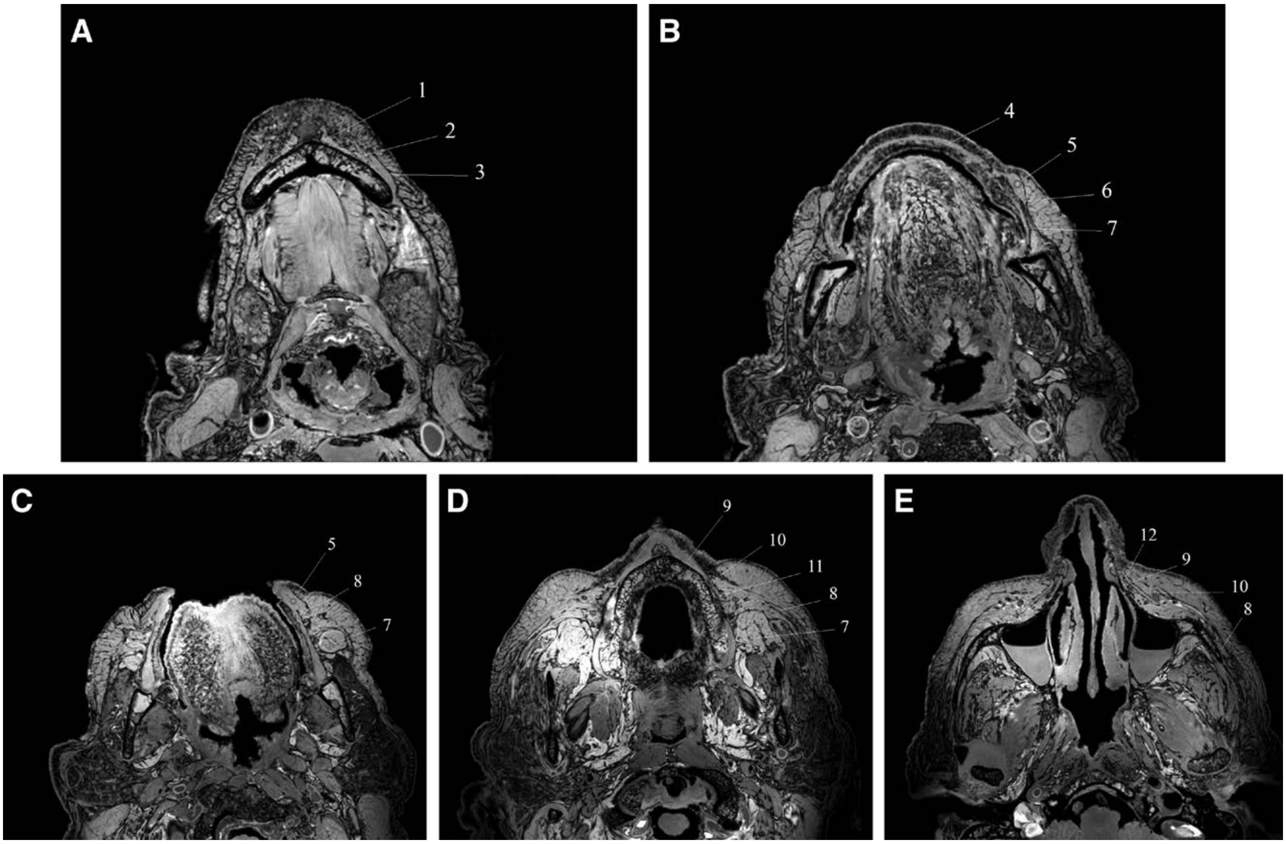

Fig. 3. Coronal. Consecutive slices from anterior to posterior in consecutive order of the 7 Tesla MRI scans (A-F). Legend of mimic muscles: 1. Nasalis muscle; 2. Levator labii superioris muscle; 3. Levator labii superioris aleque nasi muscle; 4. Orbicularis oris muscle; 5. Levator anguli oris muscle; 6. Mentalis muscle; 7. Zygomaticus muscle; 8. Modiolus region; 9. Depressor anguli oris muscle; 10. Depressor labii inferioris muscle; 11. Buccinator muscle; 12. Risorius muscle.

The clinical motive for this study was to create a basis for future research in which the mimic muscles could be identified more easily. Until today, 3D planning of osteotomies of the maxilla and mandible consists of changes of the skin surface using an iterative close point algorithm, without studying the facial muscles between bone and skin. Accurate radiological MRI knowledge of the complete course of the peri-oral mimic muscles is therefore paramount. Future research projects could focus on differences in anatomical position and vectors during the function of the mimic muscles before and after a Le Fort 1 osteotomy, before and after septonasal surgery with or without osteotomy of the nasal bone, and before and after maxillectomy. It will be helpful to both patient and surgeon to predict which specific changes in spatial anatomy of the mimic muscles result in changes in their function. The created anatomical MRI atlas and 3D model of the mimic musculature will help answer that question.

The slices of the cadaver head were made using a cryomacrotome. This cryomacrotomy technique made

Fig. 4. Example of identification of the mimic muscles in transversal direction on the cryomacrotomy photograph (A), 7 Tesla MR Image (B), and 3 Tesla MR Image (C). Legend of mimic muscles: 8. Zygomaticus muscle; 9. Levator labii superioris aleque nasi muscle; 10. Levator labii superioris muscle; 12. Nasalis muscle.

it possible to study the anatomy of the mimic muscles in detail by obtaining high-definition photographs.[16] With the use of EMAC software and an interactive image sequence viewer, a 3D model was created from the original digital photographs. This enabled a direct correlation between anatomical photographs and MRI scans.[17] Because the anatomical photographs were made from slices from a frozen cadaver head, topographic relations were well preserved and dimensions and distances could therefore be studied.[16,18] The photographs could consequently be used as the gold standard for interpreting the obtained MRI scans.

Although this cryomacrotomy technique provided a wealth of indispensable anatomical information, it meant a time-consuming process to create the gold standard reference. For this reason, the present study was performed using only one cadaver head.

The results of the present study provide evidence that separate identification of the mimic muscles is improved when imaging is performed with a 7 Tesla instead of a 3 Tesla scanner. However, definitive conclusions should be drawn cautiously from the result of the present research project, because it was performed using only one cadaver head. Further research with cadaver heads is therefore recommended to confirm the present results and to justify the transition to future in vivo research.

The knowledge acquired through the present study contributes to a better understanding of the anatomy of the peri-oral mimic muscles and the interpretation of the functional vector of these muscles on 7 Tesla MRI scans. This may improve diagnostics and may help unravel the exact mechanism behind changes in dynamics of the mimic musculature due to surgery. The results of this study can serve as a basis for future research on peri-oral mimic muscles and 7 Tesla MRI scanners.

CONCLUSIONS

The created anatomical MRI atlas presents a good overview of the exact anatomical position of the peri-oral mimic muscles from origin to insertion. The present atlas can be used for future reference. The present study demonstrates that using a 7 Tesla MRI scanner, compared with a 3 Tesla MRI scanner, considerably improves the identification of individual peri-oral mimic muscles in their course from origin to insertion. This could lead to improved diagnostics and better treatment options when used in a clinical setting. Further research is needed to validate the use of a 7 Tesla MRI scanner for identification of mimic muscle in repose and in their course of action.

Hilde Schutte, MD
Huispostnummer G05.222,
Postbus 85500
3508 GA Utrecht
The Netherlands
E-mail: hilde.n.schutte@gmail.com

ACKNOWLEDGMENTS

The head was derived from a body which had entered the department of anatomy through a donation program. Written informed consent had been obtained during lifetime, permitting the use of the entire body for educational and research purposes.

REFERENCES

1. Blair RJ. Facial expressions, their communicatory functions and neuro-cognitive substrates. *Philos Trans R Soc Lond B Biol Sci.* 2003;358:561–572.
2. Hannawa AF. "Explicitly implicit": examining the importance of physician nonverbal involvement during error disclosures. *Swiss Med Wkly.* 2012;142:w13576.
3. Nooreyazdan M, Trotman CA, Faraway JJ. Modeling facial movement: II. A dynamic analysis of differences caused by orthognathic surgery. *J Oral Maxillofac Surg.* 2004;62:1380–1386.
4. Johns FR, Johnson PC, Buckley MJ, et al. Changes in facial movement after maxillary osteotomies. *J Oral Maxillofac Surg.* 1997;55:1044–1048; discussion 1048.
5. Al-Hiyali A, Ayoub A, Ju X, et al. The impact of orthognathic surgery on facial expressions. *J Oral Maxillofac Surg.* 2015;73:2380–2390.
6. Muradin MSM, Rosenberg AJWP, van der Bilt A, et al. The effect of alar chinch sutures and V-Y closure on soft tissue dynamics after Le Fort I osteotomies: a preliminary study. *J Cranio-Maxillofac Surg* 2009;37:334–340.
7. Muradin MS, Rosenberg AJ, van der Bilt A, et al. The influence of a Le Fort I impaction and advancement osteotomy on smile using a modified alar cinch suture and V-Y closure: a prospective study. *Int J Oral Maxillofac Surg.* 2012;41:547–552.
8. Som PM, Su ANG, Stuchen C, et al. The MR imaging identification of the facial muscles and the subcutaneous musculoaponeurotic system. *Neurographics* 2012;2:35–43.
9. Farrugia ME, Bydder GM, Francis JM, et al. Magnetic resonance imaging of facial muscles. *Clin Radiol.* 2007;62:1078–1086.
10. Umutlu L, Ladd ME, Forsting M, et al. 7 Tesla MR imaging: opportunities and challenges. *Rofo.* 2014;186:121–129.
11. Kraff O, Quick HH. 7T: physics, safety, and potential clinical applications. *J Magn Reson Imaging.* 2017;46:1573–1589.
12. Kraff O, Fischer A, Nagel AM, et al. MRI at 7 Tesla and above: demonstrated and potential capabilities. *J Magn Reson Imaging.* 2015;41:13–33.
13. Oomen KP, Pameijer FA, Zwanenburg JJ, et al. Improved depiction of pterygopalatine fossa anatomy using ultrahigh-resolution magnetic resonance imaging at 7 tesla. *ScientificWorldJournal.* 2012;2012:691095.
14. Fan A, Dakpé S, Dao TT, et al. Computer methods in biomechanics and biomedical engineering. 2017;20:919–928.
15. Volk F, Karamyan I, Klingner CM, et al. Quantitative magnetic resonance imaging volumetry of facial muscles in healthy patients with facial palsy. *Plast Reconstr Surg Glob Open* 2014;2:1–9.
16. Hogan QH. Lumbar epidural anatomy. A new look by cryomicrotome section. *Anesthesiology.* 1991;75:767–775.
17. Groen GJ, Krediet AC, Moayeri N, et al. Brachial plexus sonoanatomy explained by multiplanar reformatting of digitized anatomy. *Eur J Pain Suppl.* 2010;4:303–311.
18. Moayeri N, Bigeleisen PE, Groen GJ. Quantitative architecture of the brachial plexus and surrounding compartments, and their possible significance for plexus blocks. *Anesthesiology.* 2008;108:299–304.